

# Final Report

## Local Positioning System for an Active UXO Sensor

ESTCP Project MM-0738

AUGUST 2009

Dr. I.J. Won  
**Geophex, Ltd**

Approved for public release; distribution  
unlimited.



Environmental Security Technology  
Certification Program

# Local Positioning System for an Active UXO Sensor

Final Report

ESTCP Contract No. W912HQ-07-C-0037

Geophex, Ltd., 605 Mercury Street, Raleigh, NC 27603

## Introduction

The objective of this project is to demonstrate a system capable of providing the precise relative position of an electromagnetic induction (EMI) sensor while recording data over a buried target. EMI data acquired as a function of position can be used as input into sophisticated target characterization algorithms that require spatial sampling. The basic approach is to use the active transmitter of the EMI sensor as a beacon that can be located and oriented in space relative to a set of fixed reference coils that detect the sensor transmitter field (Fig. 1).

In the course of this work, Geophex has investigated two beacon location algorithms based on this principle. The first algorithm requires beacon signals recorded by two sets of orthogonal coils to compute the  $(x, y, z)$  coordinates and the orientation of the active sensor. This approach requires a nonlinear, iterative least-squares algorithm, which is relatively computer intensive. The theoretical basis of this algorithm is reviewed in Appendix A. A photograph of the prototype positioning system is shown in Figure 2. In the photo, the two sets of three orthogonal coils are housed inside each end of the “beam.” The separation between the two sets of coils is about 1.8 meters. In this system, the beam needs to be elevated above the plane on which the sensor moves to allow flux linkage through the vertical coils (i.e., the coils whose axes point horizontally).

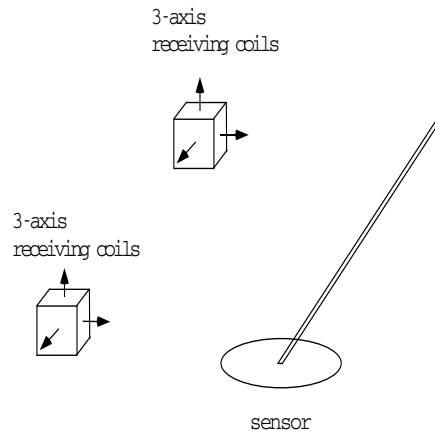


Figure 1. The primary field is detected by two sets of three orthogonal receiving coils. These six measurements are sufficient to determine the location and orientation of the sensor in three-dimensions.

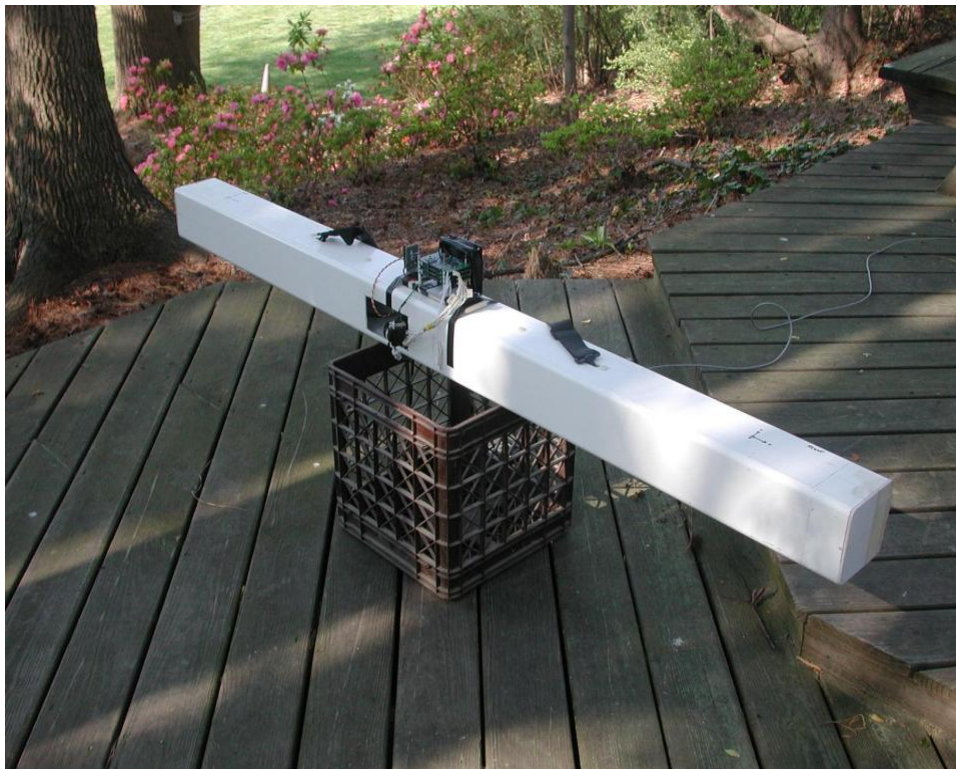


Figure 2. A set of tri-axis coils is housed inside each end of the beam.

A second, simpler algorithm has been more recently developed, which requires only three horizontal coils (axes vertical). The latter configuration assumes that the coils and the sensor are in the same horizontal plane, i.e., it solves for the  $(x, y)$  coordinates of the sensor position and assumes  $z = 0$ . The significant advantage of this algorithm is that a closed-form, analytical solution exists for computing  $(x, y)$ , which eliminates the need for an iterative algorithm. The orientation of the sensor is not computed using this approach; however, its accuracy is independent of the sensor orientation. A third (center) coil is used to normalize the end coil measurements. It can be shown that the sensor orientation dependence disappears as a result of this normalization. The only assumption is that the coils and sensor center are co-planar (although the sensor transmitting coil need not be horizontal). Simulations have shown, however, that the accuracy of the  $(x, y)$  calculation is fairly insensitive to small (e.g., 5 or 10 cm) deviations of the sensor from the plane of the three reference coils. A schematic illustration of the three-coil system and the analytic solution for the sensor coordinates are shown in Figure 3. Details of the derivation of the closed-form solution giving  $(x, y)$  in terms of the measurements can be found in Appendix B.

In a later section, results are presented using a prototype three-coil system based on this new scheme. Our original system (Figs. 1 and 2) has been extensively tested using the Geophex GEM-3 and, more recently, on signals generated using the Geonics hand-held EM-61HH sensor. Results using the EM-61HH are reported in the next section.

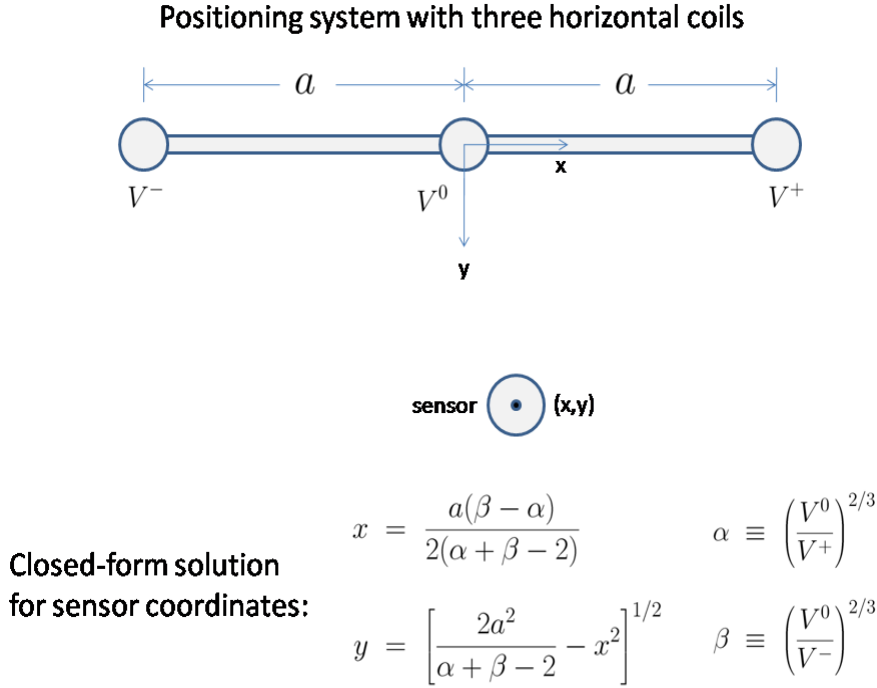


Figure 3. Schematic of the new three-coil design and the analytical solution for the  $(x, y)$  coordinates.  $V^+$ ,  $V^0$  and  $V^-$  denote the outputs of the three coils. The sensor and the three receiving coils are assumed to lie in the same plane.

### Geonics EM-61HH results

Below we present test results using our prototype positioning system (Figs. 1 and 2) to locate the EM-61HH sensor. Figure 4 shows a photo of our test setup with the EM-61HH sensor head positioned on a flat board upon which a grid of points is drawn. A closeup of the sensor head is shown in Figures 5 and 6.



Figure 4. Test setup showing the positioning system and the EM-61HH sensor head.

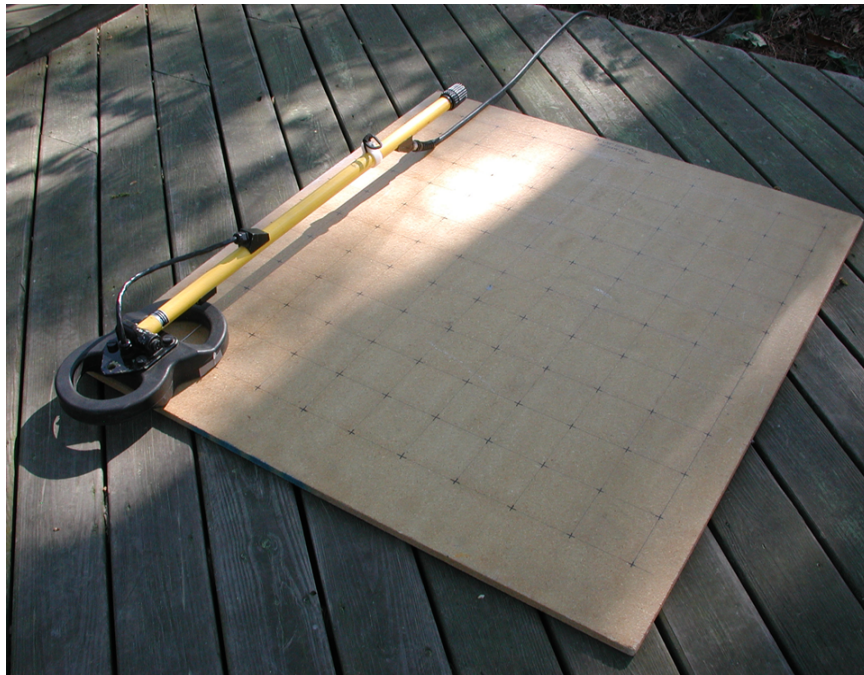


Figure 5. EM-61HH sensor head on the recording grid.



Figure 6. EM-61HH sensor head.

The EM-61HH is a time-domain instrument and the signals generated by this device consist of a train of sharp pulses with a repetition rate of about 150 Hz. A pulse train recorded over a time window of 1/30 second is shown in Figure 7. The EM-61HH signal was sampled at a rate of 192,000 Hz. The pulse train required pre-processing prior to using the positioning algorithm to provide the most accurate measurement of the signal amplitude. One approach tried was to use a peak-to-peak amplitude measurement as input into the positioning algorithm. It was found, however, that more accurate results were obtained by calculating the area under the absolute magnitude of the waveform after applying a bandpass filter to the waveform. The bandpass filtering removed a small DC component and rendered the pulse integration calculation more accurate. An FFT algorithm was used to perform the bandpass filtering. Prior to the rental of an EM-61HH sensor, our pre-processing and positioning algorithms were tested on another time-domain system (owned by Geophex), the Schiebel PSS-12, which generates a waveform that resembles that of the EM-61HH, although the Schiebel sensor operates at a somewhat slower repetition rate and lower amplitude.

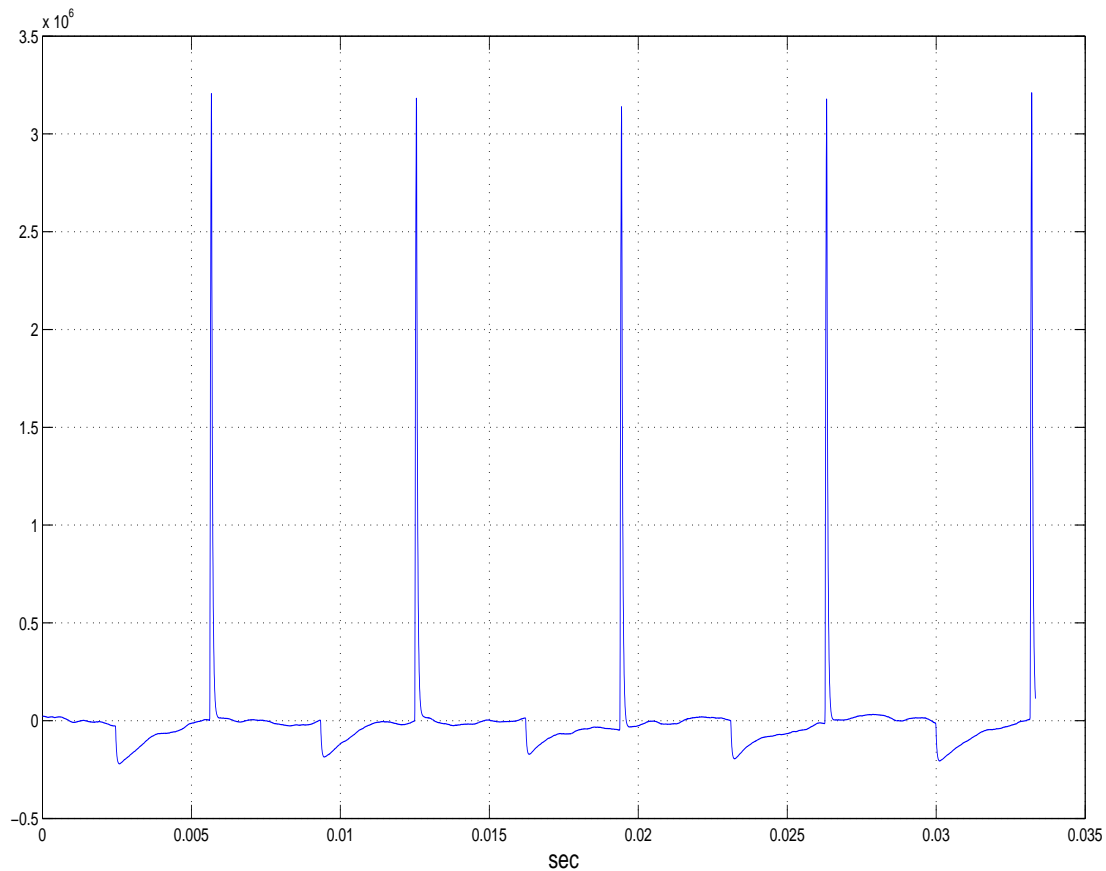


Figure 7. Waveform generated by the EM-61HH transmitter.

The transmitted signals generated by the EM-61HH were recorded over a grid of points at distances ranging from 1 to 4 meters from the positioning-system receiving coils. The positioning grid is visible in Figures 4, 5 and 6. Excellent positioning accuracy (average error less than 0.5 cm) was achieved for points between 1 and 3 m from the receiving beam. For distances beyond 3 meters the positioning accuracy began to visibly deteriorate with this system. A plot of the calculated positions is shown in Fig. 8. The dots in this figure are the calculated positions, which show excellent accuracy up to 3 meters, beyond which positioning errors are evident.

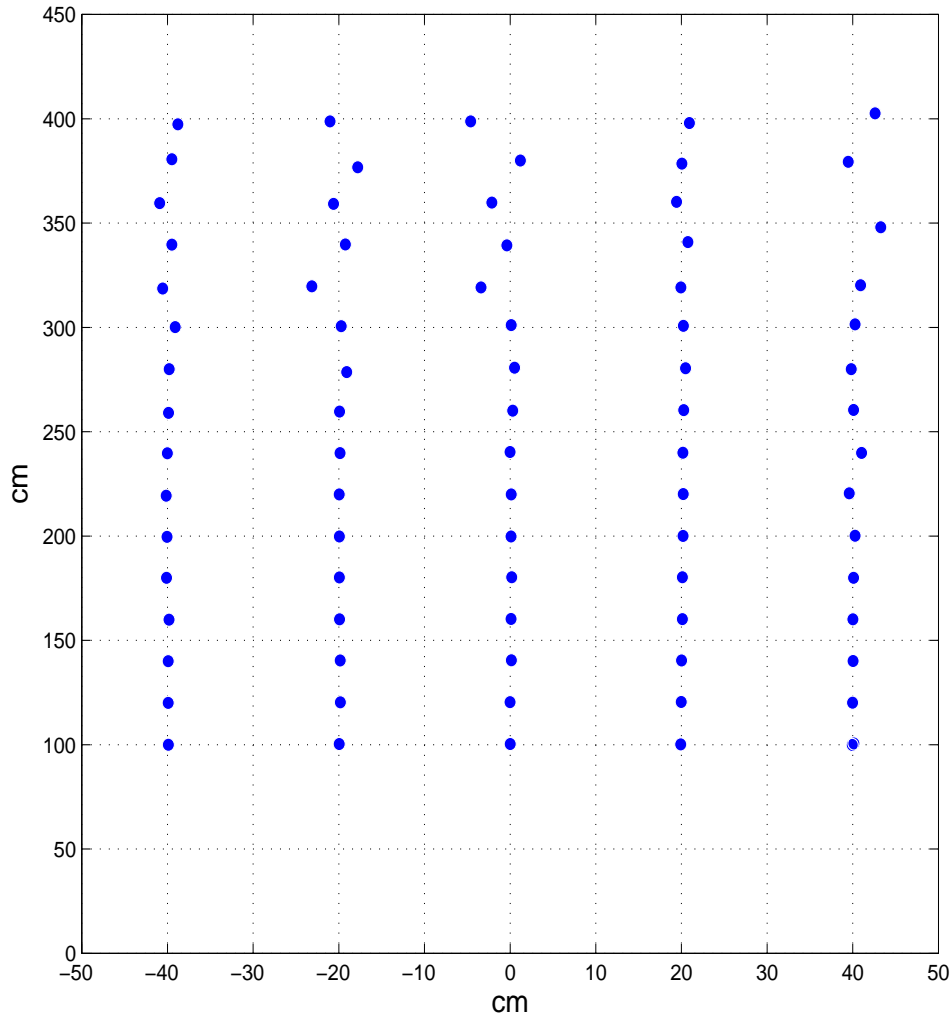


Figure 8. The dots are the computed positions. Excellent accuracy is shown out to 3 meters. Beyond 3 meters deterioration of the positioning accuracy is evident.

### Testing of the new three-coil system

Test were conducted on the three-coil system illustrated in Figure 3. Data were acquired both with the EM-61HH sensor and with the Geophex GEM-3 sensor. A new smaller (length 0.82 meters) and portable beam was constructed and appears in the foreground of the photo in Figure 9. In the background is the larger locator beam. Data were again acquired by moving the sensor on the grid shown in previous photos. The computed location using the EM-61HH sensor are shown in Figure 10 and the computed results of the GEM-3 sensor are shown in Figure 11. Aside from one point in

the upper right of Figure 10, the EM-61HH performed quite well. The results using the GEM3 appear comparable.



Figure 9. The smaller locator beam is in the lower left.

Figure 12 shows a second test of the three-coil system in which the gains of the three coils were adjusted to “force” the computed positions to coincide with the actual locations of the sensor as measured on the grid. In the figure, the circles identify the correct locations and the asterisks are the computed locations. The adjustment shown in Figure 12 was performed by slightly modifying the coil gains to minimize the mean-squared deviation of the computed locations from the actual locations. This suggests that a method could be devised to pre-calibrate the positioning system to correct for small differences in the gains of the three coils.

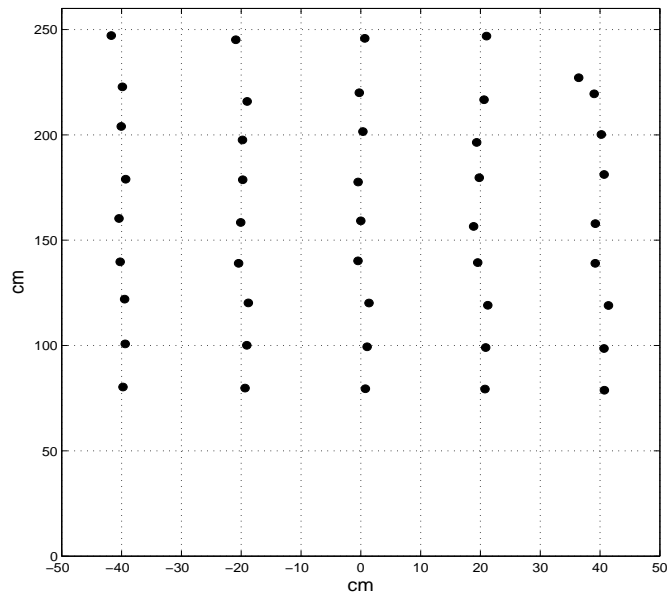


Figure 10. Computed location of EM-61HH sensor.

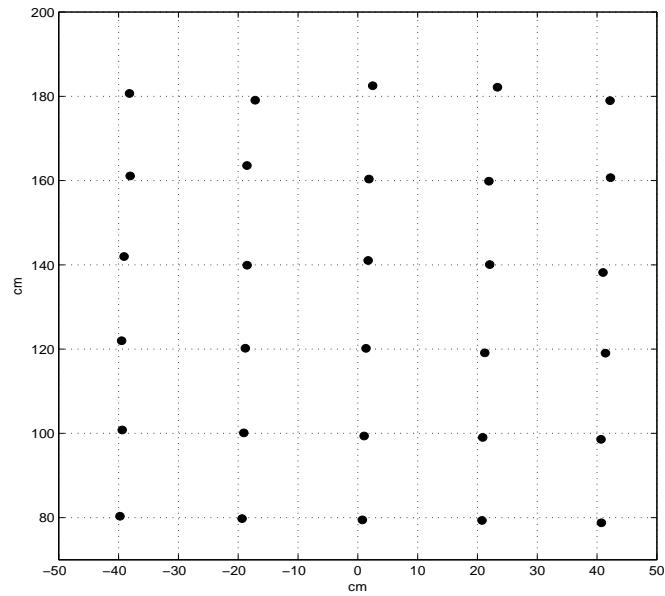


Figure 11. Computed location of GEM-3 sensor.

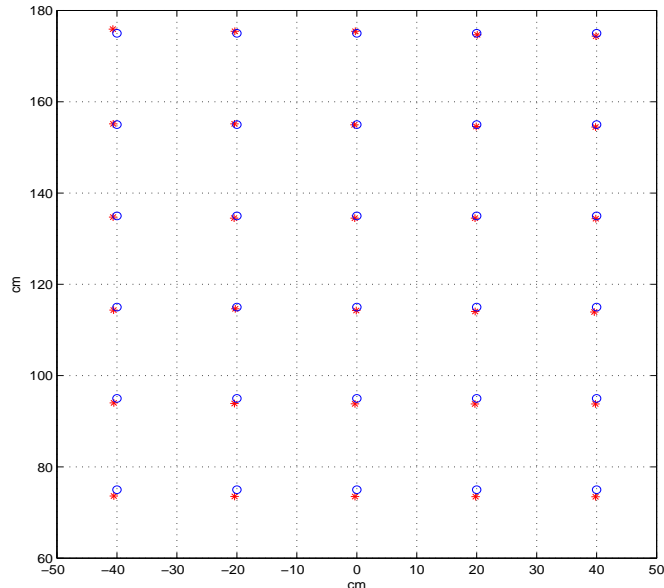


Figure 12. Computed locations of the GEM-3 sensor after calibration. The circles indicate the correct locations and the asterisks are the computed locations.

## Discussion and conclusions

Our positioning algorithms require accurate measurements of the amplitude of the sensor signal by the reference coils. Accurate estimations of this amplitude were more difficult to achieve using the EM-61HH due to the greater complexity and very short duration of the time-domain pulse compared to that of the continuous-wave GEM-3 signal. Part of the challenge in estimating the amplitude of the EM-61HH waveform is in the selection of a time window over which the amplitude integration is to be performed. The optimal duration and location of this window are more difficult to determine as the signal becomes noisier at greater sensor ranges. An advantage of the GEM-3 instrument is its excellent signal-to-noise performance, which arises from the narrowband quality of the signals. The sine and cosine multiply and integrate process performed by the GEM-3 over many cycles greatly reduces the effects of broadband noise. Broadband time-domain systems are, however, inherently more sensitive to broadband noise, although high signal levels can compensate to some extent for this sensitivity.

Results have been presented using the new analytical algorithm employing data recorded with a prototype of the three-coil system (Fig. 3 and Fig. 9). Such a system

has been constructed and tested using both EM-61HH data and GEM-3 data. Good results were obtained with both sensors, although somewhat superior positional accuracy was achieved with the GEM-3 system, which is likely due to the narrowband character of its signals and the ease of the processing of such signals, as opposed to the more complex waveforms generated by time-domain systems.

## References

1. Das Y., McFee J.E., Toews J. and Stuart G.C., Analysis of an electromagnetic induction detector for real-time location of buried objects, *IEEE Trans. Geosci. Remote Sensing* **28**, 278-288 (1990).
2. Nabighian M.N., ed., 1987. *Electromagnetic Methods in Applied Geophysics*, Vol. 1, p. 287 (Society of Exploration Geophysics).

## Appendix A: locator system 1

This system employs two sets of three mutually orthogonal receiving coils, as illustrated in Figure 1.

### A.1 Basic location equations

In this system, the two sets of orthogonal coils are elevated some distance above the sensor so that the coils with horizontal axes intercept some of the primary flux. Using a calibration procedure, accurate prior knowledge of the orientations of the six receiving coils is unnecessary, but knowledge of the relative  $(x, y, z)$  positions of each coil set is assumed known and defined relative to some convenient coordinate system with respect to which the sensor coordinates will be calculated. Simulations and field tests show, however, that the method is fairly tolerant of small errors in the positions of the receiving coils after calibration.

We model the sensor transmit coil as a magnetic dipole with dipole moment  $(M_x, M_y, M_z)$  centered at the location  $(X, Y, Z)$ . We also approximate the receiving coils as dipoles. Tests confirm that the dipole approximation is excellent for distances greater than about half a meter.

This system uses two sets of three mutually-orthogonal coils fixed at opposite ends of a rigid beam. We define an  $(x, y, z)$  coordinate system with the origin at the center of the beam, the  $x$ -axis coinciding with the beam axis (transverse direction) and the  $y$ -axis perpendicular to the beam (range direction). The centers of the two sets of coils are located at  $(-a, 0, 0)$  and  $(a, 0, 0)$ . If  $(x, y, z)$  is the location of the transmitter with dipole components  $(M_x, M_y, M_z)$ , the outputs of the three orthogonal coils are

$$V_x^\pm = \frac{A}{r_\pm^5} [(2(x \pm a)^2 - y^2 - z^2)M_x + 3(x \pm a)yM_y + 3(x \pm a)zM_z] \quad (\text{A1})$$

$$V_y^\pm = \frac{A}{r_\pm^5} [3y(x \pm a)M_y + (2y^2 - (x \pm a)^2 - z^2)M_y + 3yzM_z] \quad (\text{A2})$$

$$V_z^\pm = \frac{A}{r_\pm^5} [3z^2(x \pm a)M_x + 3zyM_y + (2z^2 - (x \pm a)^2 - y^2)M_z], \quad (\text{A3})$$

where  $r_\pm = \sqrt{(x \pm a)^2 + y^2 + z^2}$  and  $A$  is a constant. The  $+$  and  $-$  refer, respectively, to the coils at  $(a, 0, 0)$  and  $(-a, 0, 0)$ . The existing algorithm uses the six measurements  $(V_x^\pm, V_y^\pm, V_z^\pm)$  to recover the six unknowns  $(x, y, z)$  and  $(M_x, M_y, M_z)$ .

The moment components  $(M_x, M_y, M_z)$  define the orientation of the sensor, although it is convenient to use the angles  $(\theta, \phi)$  to define this orientation, where

$$M_x = M \sin \theta \cos \phi$$

$$\begin{aligned} M_y &= M \sin \theta \sin \phi \\ M_x &= M \cos \theta \end{aligned} \quad (\text{A4})$$

From the latter, the orientation of the sensor can be computed from

$$\tan \phi = M_y/M_x \quad (\text{A5})$$

$$\tan \theta = \sqrt{M_x^2 + M_y^2}/M_z \quad (\text{A6})$$

and  $M = \sqrt{M_x^2 + M_y^2 + M_z^2}$ . We shall see later that the calibration procedure allows us to define the sensor moment to be  $M = 1$ . Thus we have five unknowns to determine:  $(X, Y, Z, \theta, \phi)$ .

From reciprocity principles, one can show that the induced emf in the  $n$ -th receiving coil is given by [1]

$$V_n = \frac{i\omega\mu_0}{I} \mathbf{H}_n \cdot \mathbf{M}, \quad (\text{A7})$$

where  $\mathbf{H}_n$  is the magnetic field *generated* by the  $n$ -th receiving coil when driven with the current  $I$ . Now suppose that the  $n$ -th receiving coil has a magnetic moment,  $\mathbf{M}_n^R$ , with components  $(M_{xn}^R, M_{yn}^R, M_{zn}^R)$ , where the superscript  $R$  stands for ‘‘receiving.’’ Our calibration procedure will allow us to compute  $(M_{xn}^R, M_{yn}^R, M_{zn}^R)$  for  $n = 1, \dots, 6$  using four sensor measurements at known locations, as described below. Letting  $(X, Y, Z)$  denote the coordinates of the center of the sensor and  $(X_n, Y_n, Z_n)$  the coordinates of the center of the  $n$ -th receiving coil, define  $x_n = X - X_n$ ,  $y_n = Y - Y_n$ ,  $z_n = Z - Z_n$  and  $r_n = \sqrt{x_n^2 + y_n^2 + z_n^2}$ . With the sensor magnetic moment denoted by  $\mathbf{M}$ , one can show that the voltage induced in the  $n$ -th receiving coil is given by

$$V_n = \mathbf{M}_n^R \cdot \mathcal{H}_n \cdot \mathbf{M}, \quad (\text{A8})$$

where

$$\mathcal{H}_n \equiv \hat{x} \mathbf{H}_{xn} + \hat{y} \mathbf{H}_{yn} + \hat{z} \mathbf{H}_{zn} \quad (\text{A9})$$

is a dyadic quantity,  $\hat{x}$ ,  $\hat{y}$  and  $\hat{z}$  are Cartesian unit vectors and [2]

$$\mathbf{H}_{xn} = \frac{A}{4\pi r_n^5} [(2x_n^2 - y_n^2 - z_n^2)\hat{x} + 3x_n y_n \hat{y} + 3x_n z_n \hat{z}] \quad (\text{A10})$$

$$\mathbf{H}_{yn} = \frac{A}{4\pi r_n^5} [3y_n x_n \hat{x} + (2y_n^2 - x_n^2 - z_n^2)\hat{y} + 3y_n z_n \hat{z}] \quad (\text{A11})$$

$$\mathbf{H}_{zn} = \frac{A}{4\pi r_n^5} [3z_n x_n \hat{x} + 3z_n y_n \hat{y} + (2z_n^2 - x_n^2 - y_n^2)\hat{z}]. \quad (\text{A12})$$

Here  $\mathbf{H}_{xn}$ ,  $\mathbf{H}_{yn}$  and  $\mathbf{H}_{zn}$  are the magnetic fields generated by dipoles each of unit moment oriented, respectively, in the  $x$ ,  $y$  and  $z$  directions. In these equations,

$A = i\omega\mu_0/I$  is an unimportant constant which will be “normalized out” by the calibration procedure.

## A.2 Calibration procedure

The calibration procedure allows us to compute independently the magnetic moments,  $\mathbf{M}_n^R = (M_{xn}^R, M_{yn}^R, M_{zn}^R)$ , for all six receiving coils ( $n = 1, \dots, 6$ ) with four measurements of the sensor at four known locations. These locations were chosen to be the corners of a square with the axis of the sensor assumed vertical (in the positive  $z$ -direction). Each receiving coil is treated independently; in fact, we need not assume exact orthogonality of the coils.

To describe the procedure, suppose  $(M_x^R, M_y^R, M_z^R)$  are the moment components of one of the receiving coils. Define the magnitude of the moment of the sensor transmitter coil equal to unity ( $|\mathbf{M}| = 1$ ) and assume that the coil’s axis is vertical. Further, let  $(x_i, y_i, z_i)$ , with  $i = 1, 2, 3, 4$ , denote the (known) coordinates of the four sensor measurements and let  $V_i$  denote the corresponding outputs of the coil at these four positions. Since the sensor axis is assumed vertical (with respect to the sensor coordinate system), we obtain the following four measurements (assumed to be the corners of a square):

$$V_i = \frac{1}{4\pi r_i^5} [3z_i x_i M_x^R + 3z_i y_i M_y^R + (2z_i^2 - x_i^2 - y_i^2) M_z^R], \quad i = 1, 2, 3, 4. \quad (\text{A13})$$

This system of four equations is then solved for the three unknowns  $(M_x^R, M_y^R, M_z^R)$  using a linear least-squares algorithm. This was done using singular-value decomposition, which is also convenient for computing the condition number of the linear system. The condition number was found to be relatively small, indicating a well-conditioned system. Although only four measurements were used for calibration in our experiments, a greater number could be used in the calibration process if desired.

Define

$$\begin{aligned} x_{li} &= XL - Xcal_i \\ y_{li} &= YL - Ycal_i \\ x_{ri} &= XR - Xcal_i \\ y_{ri} &= YR - Ycal_i \end{aligned}$$

where  $i = 1, 2, 3, 4$  label the four calibration points,  $(Xcal_i, Ycal_i)$  are the coordinates of the  $i$ -th calibration point, and  $(XL, YL, ZL)$  and  $(XR, YR, ZR)$  are the coordinates of the centers of the left and right receiving coils, respectively. For the left three coils, set  $x_i = x_{li}$ ,  $y_i = y_{li}$  and  $z = ZL$  and for the right three coils set  $x_i = x_{ri}$ ,  $y_i = y_{ri}$  and  $z = ZR$ . We then solve for the moment vector for all six coils separately.

Call the three components of the moment vector  $(M_1, M_2, M_3)$  for one of the six coils. Denote the measurements from the four calibration points by  $V_i$ ,  $i = 1, 2, 3, 4$ . In the program, we call these values  $LXcal_i$ ,  $LYcal_i$ ,  $LZcal_i$ ,  $RXcal_i$ ,  $RYcal_i$  and  $RZcal_i$ ,  $i = 1, 2, 3, 4$ , where  $LX$ ,  $LY$ ,  $LZ$ ,  $RX$ ,  $RY$  and  $RZ$  label the six coils. We call the corresponding moment vectors  $MLX_j$ ,  $MLY_j$ ,  $MLZ_j$ ,  $MRX_j$ ,  $MRY_j$  and  $MRZ_j$ ,  $j = 1, 2, 3$ . To obtain  $M_j$ , we solve the overdetermined system

$$V_i = \frac{1}{r_i^5} [3z_i x_i M_1 + 3z_i y_i M_2 + (2z_i^2 - x_i^2 - y_i^2) M_3], \quad i = 1, 2, 3, 4,$$

where  $V_i$  are the measurements at the four calibration points [a factor of  $1/4\pi$  has been absorbed into  $(M_1, M_2, M_3)$ ]. For example, for the  $LX$  coil, we solve

$$\sum_{j=1}^3 F_{ij} MLX_j = B_i, \quad i = 1, 2, 3, 4,$$

using SVD, where the elements of the matrix  $F$  are given by

$$\begin{aligned} F_{11} &= 3z x_1, & F_{12} &= 3z y_1, & F_{13} &= 2z^2 - x_1^2 - y_1^2 \\ F_{21} &= 3z x_2, & F_{22} &= 3z y_2, & F_{23} &= 2z^2 - x_2^2 - y_2^2 \\ F_{31} &= 3z x_3, & F_{32} &= 3z y_3, & F_{33} &= 2z^2 - x_3^2 - y_3^2 \\ F_{41} &= 3z x_4, & F_{42} &= 3z y_4, & F_{43} &= 2z^2 - x_4^2 - y_4^2 \end{aligned}$$

and the vector  $\mathbf{B}$  is defined by

$$\begin{aligned} B_1 &= V_1 (x_1^2 + y_1^2 + z^2)^{5/2} \\ B_2 &= V_2 (x_2^2 + y_2^2 + z^2)^{5/2} \\ B_3 &= V_3 (x_3^2 + y_3^2 + z^2)^{5/2} \\ B_4 &= V_4 (x_4^2 + y_4^2 + z^2)^{5/2} \end{aligned} \tag{A14}$$

### A.3 Inversion algorithm

The outputs of the receiving coils are related to the parameters  $(X, Y, Z, \theta, \phi)$  in a nonlinear fashion through the six equations (A8). Substituting

$M_n^R = M_{xn}^R \hat{x} + M_{yn}^R \hat{y} + M_{zn}^R \hat{z}$  and  $\mathbf{M} = M_x \hat{x} + M_y \hat{y} + M_z \hat{z}$  into (A8), we obtain the six relations

$$\begin{aligned} V_n &= \frac{A}{4\pi r_n^5} \{ M_{xn}^R [(2x_n^2 - y_n^2 - z_n^2) M_x + 3x_n y_n M_y + 3x_n z_n M_z] \\ &\quad + M_{yn}^R [3y_n x_n M_x + (2y_n^2 - x_n^2 - z_n^2) M_y + 3y_n z_n M_z] \\ &\quad + M_{zn}^R [3z_n x_n M_x + 3z_n y_n M_y + (2z_n^2 - x_n^2 - y_n^2) M_z] \}, \end{aligned} \tag{A15}$$

$n = 1, \dots, 6$ , in which the moment components  $(M_{xn}^R, M_{yn}^R, M_{zn}^R)$  are obtained in the above calibration procedure. With  $(M_x, M_y, M_z)$  related to the angles  $(\theta, \phi)$  through

(A4) (with  $M = 1$ ), this gives six equations in the five unknowns ( $X, Y, Z, \theta, \phi$ ). We solve for the latter parameters using a standard Levenberg-Marquardt nonlinear least-squares algorithm.

#### A.4 Closed-form solution for EMI locator assuming zero tilts

If it is known that the axis of the sensor transmitting coil is vertical, one can derive an analytical solution for the  $(x, y, z)$  coordinates (this solution is not to be confused with that of Appendix B, where the assumption of a vertical sensor axis is not required, although that approach does not recover the  $z$  coordinate.)

We assume the origin of coordinates  $(0, 0, 0)$  is at the center of the beam. The  $(x, y, z)$  coil positions are  $(-a, 0, 0)$  and  $(a, 0, 0)$ . For zero tilts and  $(x, y, z)$  the location of the transmitter, the six coil voltages are

$$V_x^+ = \frac{3Dz(x+a)}{R_+^5} \quad (\text{A16})$$

$$V_y^+ = \frac{3Dzy}{R_+^5} \quad (\text{A17})$$

$$V_z^+ = \frac{D[2z^2 - (x+a)^2 - y^2]}{R_+^5} \quad (\text{A18})$$

$$V_x^- = \frac{3Dz(x-a)}{R_-^5} \quad (\text{A19})$$

$$V_y^- = \frac{3Dzy}{R_-^5} \quad (\text{A20})$$

$$V_z^- = \frac{D[2z^2 - (x-a)^2 - y^2]}{R_-^5} \quad (\text{A21})$$

where  $R_\pm = \sqrt{(x \pm a)^2 + y^2 + z^2}$ . Define

$$\alpha_+ \equiv \frac{V_x^+}{V_y^+} = \frac{x+a}{y} \quad (\text{A22})$$

$$\alpha_- \equiv \frac{V_x^-}{V_y^-} = \frac{x-a}{y} \quad (\text{A23})$$

This approach differs from previous approaches in that we divide by the  $y$ -coil voltages,  $V_y^\pm$ . I will argue that it is not necessarily an advantage to divide by the  $z$ -coil voltages, since, in the latter case, the final expressions are complex and involve both these ratios and their reciprocals. Defining the ratios as given by (A22) and (A23) results in the simplest closed-form solution, without a sign ambiguity in the final expression for  $z$ . In

general, we have  $V_y^\pm \rightarrow 0$  when  $z \rightarrow 0$  and  $V_x^+ \rightarrow 0$  or  $V_x^- \rightarrow 0$  when  $|x| \rightarrow a$ . We shall assume  $|z| > 0$  throughout.

Adding and subtracting (A22) and (A23) gives

$$x = a \left( \frac{\alpha_+ + \alpha_-}{\alpha_+ - \alpha_-} \right) \quad (\text{A24})$$

$$y = \frac{2a}{\alpha_+ - \alpha_-} \quad (\text{A25})$$

Note from (A22) and (A23) that  $\alpha_+ - \alpha_- > 0$  since  $y > 0$ , which will always hold. To find  $z$ , define

$$\beta_+ \equiv \frac{V_z^+}{V_y^+} = \frac{1}{3yz} [2z^2 - (a+x)^2 - y^2] \quad (\text{A26})$$

$$\beta_- \equiv \frac{V_z^-}{V_y^-} = \frac{1}{3yz} [2z^2 - (a-x)^2 - y^2] \quad (\text{A27})$$

A simple approach is to multiply  $\beta_+$  and  $\beta_-$  by  $3yz$  and subtract, giving

$$z = \frac{4a}{3(\beta_- - \beta_+)} \left( \frac{x}{y} \right) = \frac{2a(\alpha_- + \alpha_+)}{3(\beta_+ - \beta_-)}. \quad (\text{A28})$$

However, this is indeterminate at  $x = 0$ , since  $\alpha_+ = -\alpha_-$  and  $\beta_+ = \beta_-$  at  $x = 0$ . A second approach is to solve the quadratic (A26) or (A27) for  $z$ . Using (A26) gives

$$2z^2 - 3yz\beta_+ - (a+x)^2 - y^2 = 0. \quad (\text{A29})$$

Solving for  $z$  gives

$$z = \frac{3y\beta_+}{4} \pm \frac{1}{4} \sqrt{9y^2\beta_+^2 + 8[(a+x)^2 + y^2]} \quad (\text{A30})$$

Assume that  $z < 0$  (i.e., the origin of coordinates at the center of the beam is above the ground). Also,  $y > 0$  always. We shall also assume that  $y > \sqrt{2}|z|$ . If this is the case, then from (A26) and (A27),  $\beta_\pm > 0$ . Then from (A26), as  $z \rightarrow 0$ ,  $\beta_+ \rightarrow +\infty$ . This implies that we must pick the minus sign in (A30), otherwise the solution blows up as  $z \rightarrow 0$ . We thus have

$$z = \frac{3y\beta_+}{4} - \frac{1}{4} \sqrt{9y^2\beta_+^2 + 8[(a+x)^2 + y^2]} \quad (\text{A31})$$

or, alternatively, using (A27),

$$z = \frac{3y\beta_-}{4} - \frac{1}{4} \sqrt{9y^2\beta_-^2 + 8[(a-x)^2 + y^2]} \quad (\text{A32})$$

## Appendix B: locator system 2

### B.1 Closed-form solution for three horizontal-coil system

As described in the previous appendix, Locator System 1 uses two sets of three mutually-orthogonal coils fixed at opposite ends of a rigid beam. In that scheme, we define an  $(x, y, z)$  coordinate system with the origin at the center of the beam, the  $x$ -axis coinciding with the beam axis (transverse direction) and the  $y$ -axis perpendicular to the beam (range direction). In this configuration, the centers of the two sets of coils are located at  $(-a, 0, 0)$  and  $(a, 0, 0)$ . If  $(x, y, z)$  is the location of the transmitter with dipole components  $(M_x, M_y, M_z)$ , the outputs of the three orthogonal coils are

$$V_x^\pm = \frac{A}{r_\pm^5} [(2(x \pm a)^2 - y^2 - z^2)M_x + 3(x \pm a)yM_y + 3(x \pm a)zM_z] \quad (\text{B1})$$

$$V_y^\pm = \frac{A}{r_\pm^5} [3y(x \pm a)M_y + (2y^2 - (x \pm a)^2 - z^2)M_y + 3yzM_z] \quad (\text{B2})$$

$$V_z^\pm = \frac{A}{r_\pm^5} [3z^2(x \pm a)M_x + 3zyM_y + (2z^2 - (x \pm a)^2 - y^2)M_z], \quad (\text{B3})$$

where  $r_\pm = \sqrt{(x \pm a)^2 + y^2 + z^2}$  and  $A$  is a constant. The  $+$  and  $-$  refer, respectively, to the coils at  $(a, 0, 0)$  and  $(-a, 0, 0)$ . Our first algorithm uses the six measurements  $(V_x^\pm, V_y^\pm, V_z^\pm)$  to recover the six unknowns  $(x, y, z)$  and  $(M_x, M_y, M_z)$ . From the latter measurements, the orientation of the transmitter, defined by the sensor tilt angles  $(\theta, \phi)$ , can be computed from

$$\tan \phi = M_y/M_x \quad (\text{B4})$$

$$\tan \theta = \sqrt{M_x^2 + M_y^2}/M_z \quad (\text{B5})$$

The System 1 algorithm computes the parameters  $(x, y, z)$  and  $(M_x, M_y, M_z)$  from the 6-coil data set has the disadvantage of requiring a computer-intensive, nonlinear iterative scheme, which is currently performed on a laptop. We have recently derived a closed-form analytic solution for recovering the  $x$  and  $y$  sensor coordinates using only three horizontal (axes vertical) coils provided that the coils and sensor are co-planar, that is, assuming that  $z = 0$  in the above coordinate system. This new approach is described in this appendix.

This method uses a third horizontal coil at the center of the beam; that is, the three coils have coordinates  $(-a, 0, 0)$ ,  $(0, 0, 0)$  and  $(a, 0, 0)$ . In the calculations, ratios are taken between the center coil and the end coils. The significant advantage of this approach is that the solution for  $x$  and  $y$  is closed-form and thus can be calculated rapidly. If we add two additional vertical coils (with axes pointing either in the  $x$ -direction or  $y$ -direction), we also show that closed form formulas can be derived for  $M_x$  and  $M_y$ , which is sufficient for obtaining the tilt angle  $\phi$  from (B4). To obtain  $\theta$

from (B5), we also require  $M_z$ , or equivalently  $M$  since  $M_z = \sqrt{M^2 - M_x^2 - M_y^2}$ . In principle,  $M$ , the dipole moment of the transmitter, is known a priori or can be obtained with a single calibration measurement, in which case  $\theta$  can also be obtained.

As noted, this approach assumes  $z = 0$  and thus will be subject to error if the sensor deviates from the plane of the coils. However, simulations have shown that the computed values of  $(x, y)$  are fairly insensitive to small out-of-plane deviations of the sensor (e.g.,  $-5 \text{ cm} < z < 5 \text{ cm}$ ).

### Closed-form solution for $x$ and $y$

Consider a locator with three identical horizontal coils at coordinates  $(-a, 0, 0)$ ,  $(0, 0, 0)$  and  $(a, 0, 0)$ , with outputs denoted by  $V_z^-$ ,  $V_z^0$  and  $V_z^+$ , respectively. If we set  $z = 0$  in (B3), then the outputs of the three coils reduce to

$$V_z^+ = -\frac{AM_z}{[(x+a)^2 + y^2]^{3/2}} \quad (\text{B6})$$

$$V_z^0 = -\frac{AM_z}{[x^2 + y^2]^{3/2}} \quad (\text{B7})$$

$$V_z^- = -\frac{AM_z}{[(x-a)^2 + y^2]^{3/2}}. \quad (\text{B8})$$

Thus, when  $z = 0$ , the dependence on  $M_x$  and  $M_y$  disappears (i.e., the results are insensitive to the sensor tilt). For the case in which all coils are horizontal and co-planar,  $A = i\omega\mu_0NA_R/4\pi$ , where  $N$  and  $A_R$  are the turn number and area of the receiving coil. Now define the ratios

$$\alpha \equiv \left(\frac{V_z^0}{V_z^+}\right)^{2/3} = \frac{(x+a)^2 + y^2}{x^2 + y^2} \quad (\text{B9})$$

$$\beta \equiv \left(\frac{V_z^0}{V_z^-}\right)^{2/3} = \frac{(x-a)^2 + y^2}{x^2 + y^2}. \quad (\text{B10})$$

Defining  $R^2 = x^2 + y^2$ , (B9) and (B10) may be written

$$R^2 + 2ax + a^2 = \alpha R^2 \quad (\text{B11})$$

$$R^2 - 2ax + a^2 = \beta R^2 \quad (\text{B12})$$

Subtracting and solving for  $x$  gives

$$x = \frac{1}{4a}(\alpha - \beta)R^2. \quad (\text{B13})$$

Substituting  $x$  into (B11) or (B12) and solving for  $R^2$ , we get

$$R^2 = \frac{2a^2}{\alpha + \beta - 2}. \quad (\text{B14})$$

Substituting this back into (B13) gives

$$x = \frac{a(\alpha - \beta)}{2(\alpha + \beta - 2)}. \quad (\text{B15})$$

$y$  is obtained by substituting (B15) for  $x$  into (B14), recalling that  $R^2 = x^2 + y^2$  and solving for  $y$ :

$$y = \left[ \frac{2a^2}{\alpha + \beta - 2} - x^2 \right]^{1/2}, \quad (\text{B16})$$

with  $x$  given by (B15). Note that  $y$  will always be a positive number, whereas  $x$  can be positive or negative.

### Recovering the tilt of the sensor

When  $z = 0$ , we can recover the sensor moment components  $(M_x, M_y)$  once  $x$  and  $y$  have been computed if we have two additional vertical coils. The output of two vertical coils at the ends of the beam whose axes are oriented, respectively, in the  $x$ -direction or  $y$ -direction are given by setting  $z = 0$  in (B17) and (B18)

$$V_x^\pm = \frac{A}{\rho_\pm^5} [(2(x \pm a)^2 - y^2)M_x + 3(x \pm a)yM_y] \quad (\text{B17})$$

$$V_y^\pm = \frac{A}{\rho_\pm^5} [3y(x \pm a)M_x + (2y^2 - (x \pm a)^2)M_y], \quad (\text{B18})$$

where  $\rho_\pm \equiv \sqrt{(x \pm a)^2 + y^2}$ . Once  $x$  and  $y$  have been computed from (B15) and (B16), either (B17) or (B18) defines a 2 by 2 linear system that can be solved for  $(M_x, M_y)$ . For example, from (B17), the data consist of  $(V_x^+, V_x^-)$ .